

Oil & Natural Gas Technology

DOE Award No.: ESD12-011

Topical Report

Properties of Hydrate-Bearing Sediments Subjected to Changing Gas Compositions

Submitted by:

Timothy Kneafsey, Project PI
Lawrence Berkeley National Laboratory
1 Cyclotron Road
Berkeley, CA 94720

Prepared for:

United States Department of Energy
National Energy Technology Laboratory



Office of Fossil Energy

**Behavior of methane hydrate when exposed to a 23% carbon dioxide -77% nitrogen gas
under conditions similar to the ConocoPhillips 2012 Ignik Sikumi Gas Hydrate Field Trial**

Topical Report

Timothy J. Kneafsey

Seiji Nakagawa

Sharon E. Borglin

February 5, 2013

ESD12-011

Tasks 2.0 and 3.0

Lawrence Berkeley National Laboratory

1 Cyclotron Road

Berkeley, CA 94720

DISCLAIMER* -- The Disclaimer must follow the title page, and must contain the following paragraph:

“This report was prepared as an account of work sponsored by an agency of the United States Government. Neither the United States Government nor any agency thereof, nor any of their employees, makes any warranty, express or implied, or assumes any legal liability or responsibility for the accuracy, completeness, or usefulness of any information, apparatus, product, or process disclosed, or represents that its use would not infringe privately owned rights. Reference herein to any specific commercial product, process, or service by trade name, trademark, manufacturer, or otherwise does not necessarily constitute or imply its endorsement, recommendation, or favoring by the United States Government or any agency thereof. The views and opinions of authors expressed herein do not necessarily state or reflect those of the United States Government or any agency thereof.”

Executive Summary

We have performed a series of carefully controlled laboratory tests in which we monitor changes in methane hydrate-bearing samples when a nitrogen/carbon dioxide gas mixture is flowed through. This was done to provide additional background information for a field test that was performed in which the same mixture of carbon dioxide and nitrogen was injected into a methane hydrate-bearing unit beneath the north slope of the Brooks Range in northern Alaska (ConocoPhillips 2012 Iñik Sikumi gas hydrate field trial).

In the tests we report on here, we have measured the kinetic gas exchange rate for different hydrate saturations and different test configurations to provide an estimate for comparison to numerical models. In our tests, the exchange rate decreased over the course of time during the tests as methane was depleted from the system. Following the passing of the methane front, the exchange rate ranged from 3.8×10^{-7} moles methane/(mole water*s) to 5×10^{-8} moles methane/(mole water*s). In these rates, the moles of water refers to water originally held in the hydrate.

We monitored permeability, or permeability proxy to monitor changes due to gas exchange. We observed permeability increases and decreases as the gas exchange occurs. Using our Split Hopkinson Resonant Bar apparatus, we observed changes in the physical strength of the hydrate-bearing sand during exposure to the mixed gas. Upon introduction of the mixed gas, the sample became less stiff and wave attenuation increased, indicating the presence of liquid water between mineral grains and hydrate. Slow dissociation of the hydrate showed a range of hydrate stability conditions as the gas composition changed from dissociation and dilution of the previously injected nitrogen.

Goals and Objectives

The objective of this work is to measure physical, chemical, mechanical, and hydrologic property changes in methane hydrate bearing sediments subjected to injection of carbon dioxide and nitrogen. Because the replacement of methane by carbon dioxide and nitrogen is thermodynamically favored in some cases, these gases are considered to enhance the extraction of methane from hydrate, and to simultaneously sequester carbon dioxide. DOE has participated in a field test in Alaska in which nitrogen and carbon dioxide were introduced into a methane hydrate-bearing reservoir, and then gas was extracted. Analysis and modeling of the data and processes observed are expected to be performed for some time resulting in questions that can be efficiently answered in the laboratory. We will make measurements that support these investigations. We will share our results with those analyzing the field test, and the scientific community, and communicate with those analyzing the field test to ensure our tests are on target to answer their questions.

Technical Highlights, Results, and Discussion

Abstract

We have performed a series of carefully controlled laboratory tests in which we monitor changes in methane hydrate-bearing samples when a nitrogen/carbon dioxide gas mixture is flowed through. This was done to provide additional background information about a field test that was performed in which a mixture of carbon dioxide and nitrogen was injected into a methane hydrate bearing unit beneath the north slope of the Brooks Range in northern Alaska (ConocoPhillips 2012 Igñik Sikumi gas hydrate field trial). We have measured the kinetic gas exchange rate for our tests, providing an estimate for comparison to numerical models. In our tests, the exchange rate decreased over the course of the tests as methane was depleted from the system, but following the passing of the methane front, the exchange rate ranged from 3.8×10^{-7} moles methane/(mole water*s) to 5×10^{-8} moles methane/(mole water*s). In these rates, the moles of water refers to water originally held in the hydrate. We observed permeability increases and decreases as the gas exchange occurs. Using our Split Hopkinson Resonant Bar apparatus, we have observed changes in the physical strength of the hydrate-bearing sand during exposure to the mixed gas. Slow dissociation of the hydrate showed a range of hydrate stability conditions as the gas composition changed from dissociation and dilution of the injected nitrogen.

Table of Contents

Abstract	6
Knowledge of State of the Art	8
Experimental setup	9
Flow-through tests.....	9
Flow-through test with geophysical and X-ray CT monitoring.....	10
Results	13
Flow-through tests.....	13
Permeability Changes	15
Flow-through test with geophysical and X-ray CT monitoring.....	16
Hydrate Formation.....	16
Gas Exchange	18
Dissociation	21
Discussion	27
Risk Analysis	29
Milestone Status	30
Schedule Status	30
Cost Status	30
Conclusions	31
References	33

Knowledge of State of the Art

A number so studies have been carried out investigating the impact of injecting carbon dioxide (CO₂) and CO₂-nitrogen (N₂) mixtures into methane hydrate for the purposed of sequestering CO₂ and releasing methane (CH₄) (Adisasmito et al., 1991; Anderson et al., 2003; Lee et al., 2003; Linga et al., 2007; Lu et al., 2007; Ota et al., 2005a; Ota et al., 2005b; Ota et al., 2007; Park et al., 2006; Seo et al., 2001), and review articles have been published summarizing the literature (Goel, 2006; Nago and Nieto, 2011; Zhao et al., 2012). Most of the studies that have been performed have investigated the fundamental physical/chemical nature of the exchange of CO₂ and/or N₂ with CH₄ in the clathrate. These studies have been beneficial in identifying the limits to the effectiveness of CO₂ injection into CH₄ hydrate for the purposes of CH₄ production, and CO₂ sequestration. CO₂ is thought to replace CH₄ from the large cages of the hydrate structure, but because of its size, is less well suited to replace the CH₄ from the small cages. This limits CH₄ replacement to 64% (Lee et al., 2003; Lee and Collett, 2005; Park et al., 2006). Coinjection of CO₂ (20 mole %) with N₂ increases CH₄ replacement to 85%, as the nitrogen can occupy the small cages of the hydrate cell. Park et al., (2006) point out that using the nitrogen implies that CO₂ from flue gas from a power plant would not have to be separated out prior to injection. These studies have used NMR and Raman spectroscopy to understand both the location of the guest molecules (CO₂, CH₄, N₂) in the hydrate, and to examine the kinetics of replacement. Regarding the kinetics, the replacement of CH₄ in hydrate appears to be rapid (timescale of minutes) for powdered hydrate in well-mixed systems, however the replacement rate declines with time indicating that chemical kinetics may be much faster than mass transfer limitations within solid hydrate.

Few studies have examined the hydrologic and physical/mechanical property changes that occur during a hydrate composition change (eg. Nakagawa and Kneafsey unpublished data 2009, Stevens et al., 2008). Nakagawa and Kneafsey observed resonance properties of CH₄ hydrate bearing sand when CO₂ was introduced. In spite of the CH₄ hydrate reaction appearing to be complete prior to CO₂ introduction, the sample became significantly stiffer immediately after the CO₂ was injected indicating additional hydrate was formed providing additional cementation in their unsaturated sample. They did not measure hydrologic properties in this test, and quantification of the effluent gas was crude. Stevens et al. (2008) measured the permeability of CH₄ hydrate bearing sandstone when CO₂ was flowed through, finding that the permeability was not significantly changed over the limited number of conditions tested. In spite of the obvious value of these studies, they were performed over a limited range of conditions (mostly dry hydrate) and fail to address important reservoir issues such as pressure increase upon injection and effect of gas composition change in a varying composition system.

In FY 12, a mixture of N₂ and CO₂ were injected into a wet CH₄ hydrate-bearing reservoir in Alaska to field-test the concept of enhanced gas production and CO₂ sequestration. Modeling studies and laboratory studies have been performed to predict the effectiveness of this injection and subsequent withdrawal of gas. Following the test,

analysis of the data and occurrences are occurring. Here, we investigated processes associated with the injection of a mixture of CO₂ and N₂ gases into CH₄ hydrate bearing porous media under flow-through conditions. We measured effluent gas compositions using gas chromatography. We quantified the exchange kinetics of the N₂ and CO₂ replacement into CH₄ hydrate using flow through reactors and breakthrough curve analysis. Permeability was measured to detect changes, and geophysical property changes were measured using the Split Hopkinson Resonant Bar apparatus.

Experimental setup

Flow-through tests

For the tests reported here, fine-grain silica sand (F110 U.S. Silica, grain size <110 μ m) was uniformly moistened with distilled, de-ionized water to either 20% or 40% water saturation and compacted to 0.41 porosity in a cylindrical, stainless steel column with inner diameter of 1 cm and length of 25 cm (Figure 1). The cylinder was sealed and placed in a water bath at 4°C and pressurized to 4.83 MPa (700 psi) with CH₄. Temperature and pressure of the system, as well as pressure differential across the length of the column were recorded every 20 seconds. Hydrate was allowed to form for at least 24 hrs at 4.83 MPa and 4°C. Prior to starting flow of mixed gas, a permeability test was completed by flowing CH₄ through the column at rates ranging from 0 to 10 ml/min and recording change in differential pressure.

To perform flow-through gas exchange tests, the pressure in the system was increased with CH₄ to 9.66 MPa (1400 psi). This gas was then replaced at the column inlet by a mixture of 77% N₂ and 23% CO₂. This gas mix was set to flow through the column at a constant rate of 0.1 mL/min. Pressure and flow were maintained using high-pressure ISCO syringe pumps at the inlet and outlet of the system. Once flow commenced, gas composition was monitored by sampling and analyzing outlet gas. To allow for gas sampling, a 0.2 mL sampling tube was added to the effluent tubing. This sampling tube was manually actuated. First, the tube and expansion chamber were evacuated, followed by sampling 0.2 ml from the effluent line, expanding the 0.2 ml of gas into an evacuated 1-2 ml volume having a septum allowing sampling. Gas analysis was performed using a Shimadzu 8A gas chromatograph with a thermal conductivity detector. Both externally procured and laboratory-made standards were used for calibration.

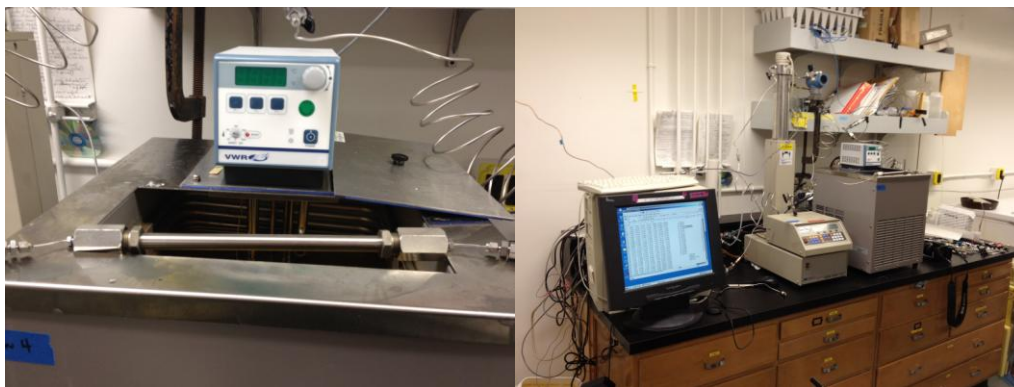


Figure 1. Experimental setup for flow-through tests. Picture (a) is a close up of the column containing the hydrate, (b) shows the outlet syringe pump and data acquisition system.

Flow-through test with geophysical and X-ray CT monitoring

Fine-grain silica sand (F110 U.S. Silica, average grain size $\sim 110 \mu\text{m}$) was uniformly moistened with distilled, de-ionized water and compacted to 0.39 porosity in a cylindrical, 0.5 mm-thick PVC jacket. The resulting sample [7.67 cm long and 3.81 cm diameter with a water saturation of 0.19 (fraction of porespace filled with water)] was installed in the Split Hopkinson Resonance Bar (SHRB) apparatus (Figure 2). It was desired to create a sample in which the hydrate cemented the mineral grains together, yet was present in a limited quantity such that small changes to the hydrate would be indicated by the geophysics. This sacrificed some of the ability to extract information from the test using X-ray CT, and increased the difficulties in obtaining mass balance.

A 14.5 MPa (2100 psi) absolute pressure isotropic confining stress was applied to the sample using compressed N₂ gas and the sample was cooled to about 4°C, to allow CH₄ hydrate formation by pressurizing the porespace using pure CH₄ gas to 9.66 MPa (1400 psi). The gas consumption and temperature of the pump barrel were recorded over time to allow quantification of the hydrate formed. After the start of hydrate formation was confirmed by resonance frequency and attenuation changes, hydrate formation was left to continue for about 3 days. After three days, flow of CH₄ gas was attempted through the sample. No flow was possible even under extreme conditions (6 MPa pressure differential), so the pressure at the sample outlet was reduced slowly to a value beneath the hydrate stability point until flow was established. Upon establishing flow, the pore pressure was reset to 9.66 MPa, and the system was allowed to equilibrate for 15 hours and it remained permeable.

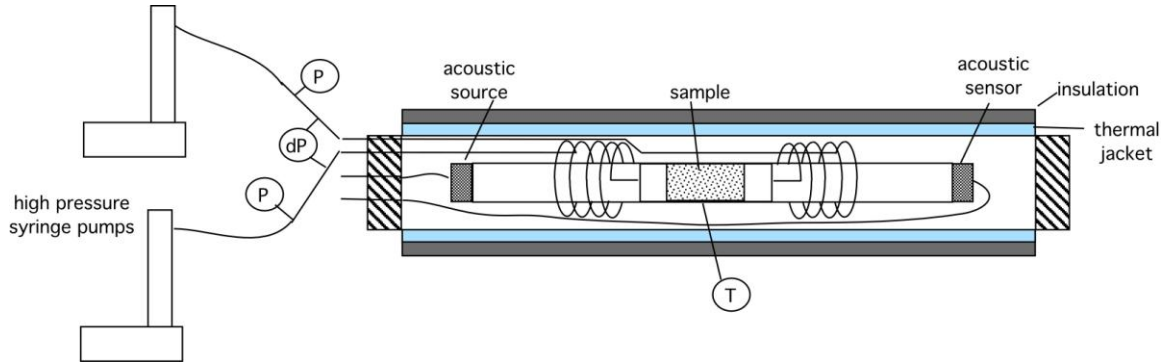
Because the Split Hopkinson Resonance Bar apparatus (SHRB) internally uses extended lengths of coiled narrow tubing to minimize impacts on resonance, exact quantification of permeability is difficult. It is possible, however, to monitor changes in permeability by measuring the pressure differential across the sample and tubing while flow occurs. To that end, differential pressure was monitored using a Rosemount 3051 pressure transmitter.

As in the flow-through tests described above, to allow for gas sampling, a 0.2 mL sampling tube was added to the effluent tubing. This sampling tube was manually actuated, by first evacuating the tube and expansion chamber, then sampling 0.2 ml from the effluent line and expanding the 0.2 ml of pressurized gas into an evacuated 1-2 ml volume having a septum allowing sampling. Gas analysis was performed using a Shimadzu 8A gas chromatograph with a thermal conductivity detector. Both externally procured and laboratory-made standards were used for calibration.

Following hydrate formation and equilibration, a mixture of CO₂ (23%) and N₂ (77%) was introduced and flowed through the hydrate-bearing sand. The flow rate was 30

ml/hour, roughly 1 (0.88) pore volumes per hour. After three days of flow, the inlet to the sample was closed, and the hydrate sample was slowly dissociated by increasing temperature at constant pressure.

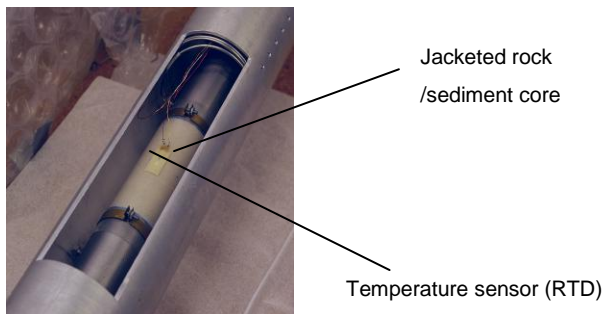
In addition to monitoring pressure, temperature, and gas composition, sample resonance properties (frequency and attenuation) were monitored, and spatially-resolved sample density was intermittently monitored using X-ray computed tomography.



a. Experiment schematic showing Split Hopkinson Resonant Bar.



b. Gas confining cell (top right) and a suspension cage (front) housing the sample-bar assembly



c. Jacketed sample core placed between steel extension rods



d. Source and receiver units attached to the ends of the bars. Note that these units were potted with high-strength epoxy for protection later.

Figure 2. SHRB system setup.

Resonance frequencies and attenuations of extension and torsion mode vibrations of the sample were measured during the experiment using a modified resonant bar technique (Nakagawa, 2011)(See Figure 3). From these measurements and the sample geometry and density, P and S-wave velocities and attenuations are determined. This technique allows use of a small cylindrical core for seismic property measurements at frequencies which would require meter-long samples if a conventional resonant bar technique was used.

Before the experiments with hydrate were started, the packed moist-sand sample was isotropically compressed in the pressure vessel twice up to 14.5 MPa (2,100 psi) to minimize the compaction-induced changes in the mechanical properties during the experiment. The changes in the measured resonance frequencies during hydrate formation, replacement, and dissociation experiments were between 600 Hz and 1.6 kHz for the extension mode, and 400 Hz and 1.05 kHz for the torsion mode. Increases in the resonance frequencies were caused primarily by the cementation of sand grains by CH₄ hydrate. Concurrent CT scans were conducted to examine formation, dissociation, and heterogeneity of hydrate in the sample.



Figure 3. Experimental setup

Results

Flow-through tests

In this sequence of experiments the column was packed with sand at either 20 or 40% initial water saturation and placed under CH₄ hydrate-forming conditions, 4°C and 4.83 MPa (700 psi). After hydrate formation, pressure was increased to 9.66 (1400 psi) using CH₄ gas, which was then exchanged for a 77% N₂/23% CO₂ mixture at a flow rate of 0.1 ml/min.

Gas measurements for the 20% initial water saturation test (Figure 4) show close to 100% CH₄ in the effluent for 2 hrs, after which CH₄ concentration decreased sharply until the experiment was stopped due to low CH₄ detection after 80 hours (60 pore volumes). N₂ and CO₂ concentrations approached the inlet gas composition, with the CO₂ concentration lagging a bit behind the N₂ concentration presumably due to interaction or exchange with the hydrate. Gas measurements for the 40% saturated column also show close to 100% CH₄ in the effluent at the beginning of the test but begin to decrease immediately, and as in the 20% saturated column the N₂ and CO₂ concentrations approached the inlet gas composition. The more sudden decrease in CH₄ concentration is likely due to the smaller gas volume in the sample from the higher initial water saturation.

Gas exchange rates were calculated for both tests. The rates presented are in units of moles of CH₄ exchanged per second, per mole of water initially present in the system and assumed to be completely present in the resulting hydrate. Both columns had an exchange rate of 3.8×10^{-7} moles CH₄/(mole H₂O*s) at 3 hrs, but the 20% column maintained a higher rate, reaching 1.5×10^{-7} moles CH₄/(moles H₂O*s) at 80 hrs, while the 40% column dropped to 5.0×10^{-8} moles CH₄/(moles H₂O*s). The average exchange rate for this period was 2.82×10^{-7} moles CH₄/(moles H₂O*s) for the 20% column and 1.53×10^{-7} moles CH₄/(moles H₂O*s) for the 40% column. The values for gas exchange rates are shown in Figure 5. The 40% initial water saturation column, while having more hydrate and CH₄ present, may also have more rapid flow through the column, and any heterogeneity may induce preferential gas flow reducing contact area with the incoming exchange gas. This could be responsible for the lower rate.

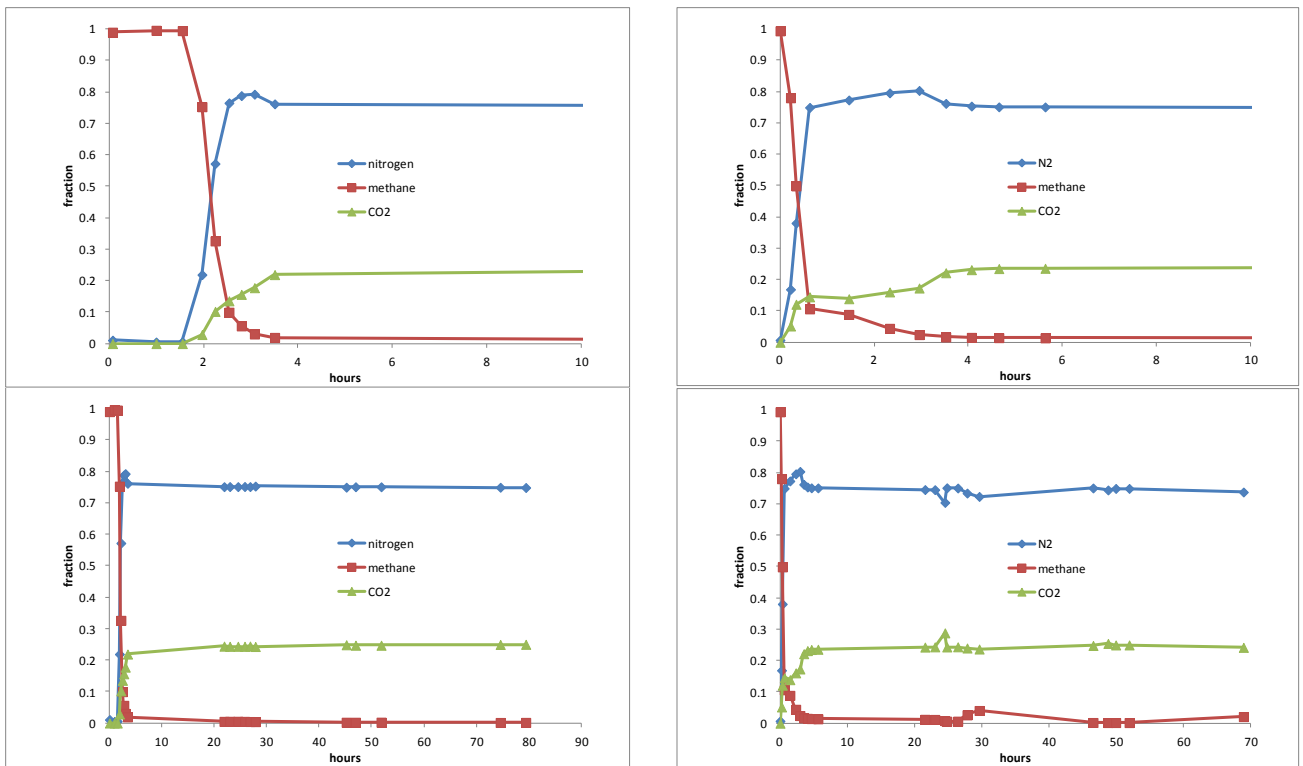


Figure 4. Gas composition during gas exchange, 20% saturation. Left panel, 20% initial water-saturation, right panel is 40% initial water saturation. Top shows 0-10 hours, lower entire gas exchange experiment.

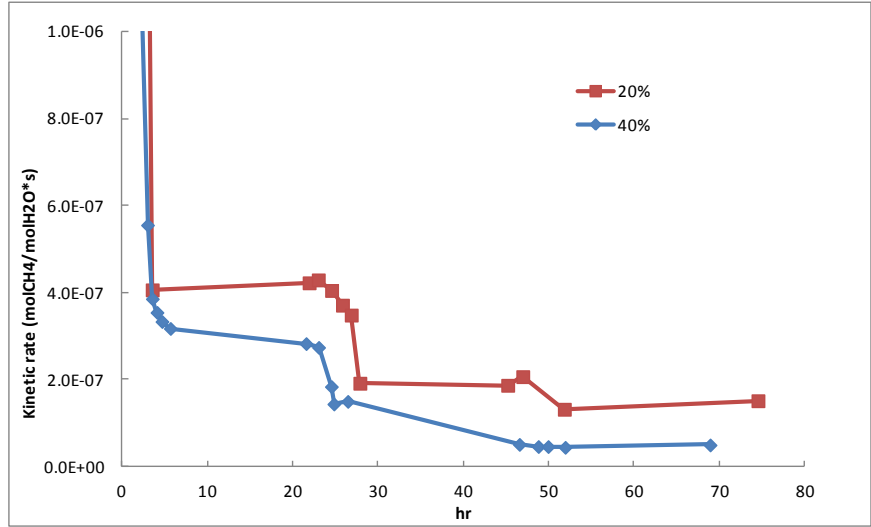
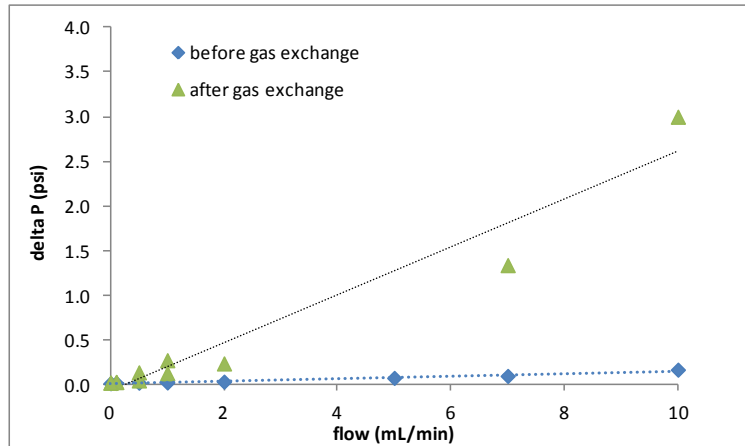


Figure 5. Gas exchange rates between CH₄ hydrate and N₂/CO₂ gas mixture, 1400 psig, 20% and 40% initial water saturation sand.

Permeability Changes

Column permeability was measured before and after gas exchange and is shown below in Figure 6. Permeability was measured by varying flow rate and monitoring the differential pressure across the column. Before the gas exchange test permeability was measured at 4.83 MPa (700 psig), after the gas exchange test the permeability was measured at 9.66 MPa (1400 psig). The increase in slope of the line increased indicates the permeability of the column decreased as a result of the gas exchange test. Permeability calculations (adjusted for differences in pressure) for before and after gas exchange for both the 20% and 40% are shown in Figure 6 relative to flow rate through the column. Average permeability changes from $5.73 \times 10^{-11} \text{ m}^2$ to $2.23 \times 10^{-11} \text{ m}^2$ for the 20% column and $1.00 \times 10^{-10} \text{ m}^2$ to $1.29 \times 10^{-11} \text{ m}^2$ for the 40% column. No water was produced in these tests.



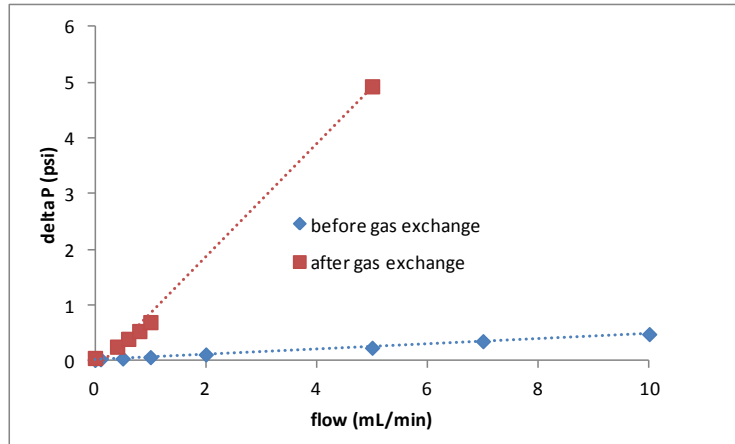


Figure 6. Permeability changes due to the gas exchange test. Top is 20% initial water-saturation sand column, lower 40% initial water saturation.

Flow-through test with geophysical and X-ray CT monitoring

The experimental results will be presented in three sub sections corresponding to the three experiments – hydrate formation, gas exchange, and hydrate dissociation. No water was produced in these tests.

Hydrate Formation

Pressure, Temperature, Differential Pressure

CH₄ hydrate was formed using a chilled sample at constant pressure. Upon pressurization (red arrow in Figure 7), the sample temperature increased in response to the increase in pressure. The temperature declined over the next several hours, and the hydrate formation did not show a strong temperature signal. Although the circulating bath temperature was well-controlled, sample temperature variations occurred in response to strong room temperature fluctuations (blue arrow in Figure 7). One indication that hydrate formed is the differential pressure response to room temperature. A hydrate plug at some location in the sample or line formed, resulting in wildly sweeping pressure differentials across the sample (yellow arrow in Figure 7). Conductivity was reestablished by depressurization of the downstream side to immediately below the hydrate stability pressure at the prevailing temperature and waiting for the pressure to equalize. Upon equalization, the sample was repressurized and allowed to equilibrate for 15 hours.

Because of the narrow tubing used in the SHRB, the measured pressure differential provides an indication of the permeability with lower differential pressure indicating higher permeability. A flowrate of 0.5 mL/min induced a pressure differential of 1.1 psi in the CH₄ hydrate-bearing sample.

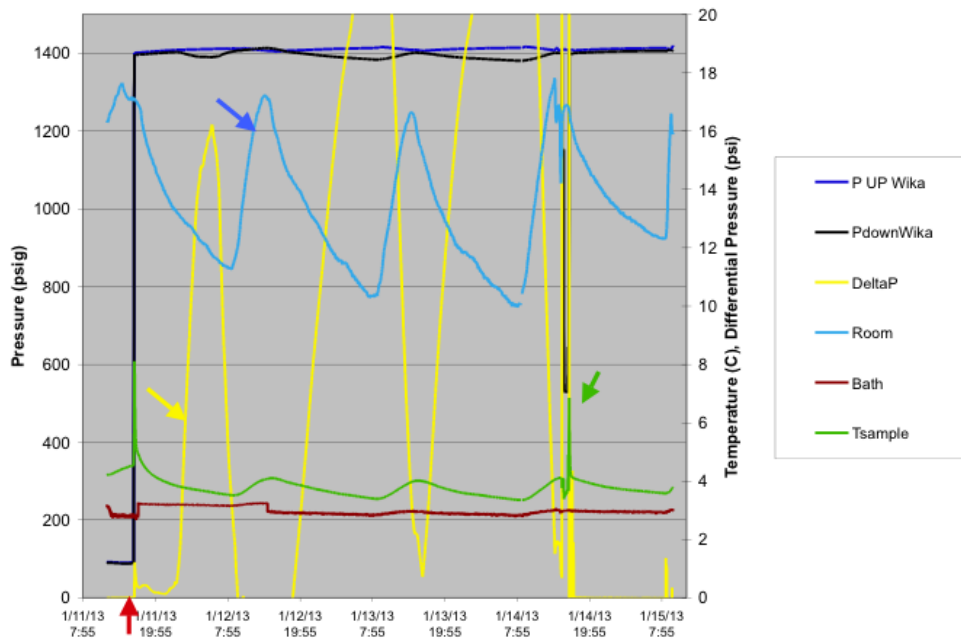


Figure 7. Physical conditions during CH4 hydrate formation.

Gas Composition

No data are presented here because only CH4 was used in this portion of the test.

Seismic Properties

A summary of the seismic measurements for the CH4 hydrate formation are shown in Figure 8. The initial P and S-wave velocities (V_P , V_S) of the sample (without hydrate) at an effective confining stress of 700 psi were 976 m/s and 658 m/s, and attenuations (a_P , a_S) 0.09% and 0.21%, respectively. The Poisson ratio ν from the velocity ratio was 0.085. Introducing CH4 gas in the sample immediately resulted in increases in both velocities and attenuations, indicating the formation of CH4 hydrate at the grain contacts. The attenuations reached a peak one to two hours after the start of hydrate formation, at about 2.5%. The Poisson ratio also reached its peak value of ~ 0.3 at the same time. Most of the hydrate formation occurred within the first 24 hours of the experiment. However, small increases in the velocities were observed at up to 72 hours after the hydrate replacement test was started. The velocities, attenuations, and the Poisson ratio at the final state were $V_P=3,236$ m/s, $V_S=2026$ m/s, $a_P=0.54\%$, $a_S=0.64$, and $\nu=0.18$.

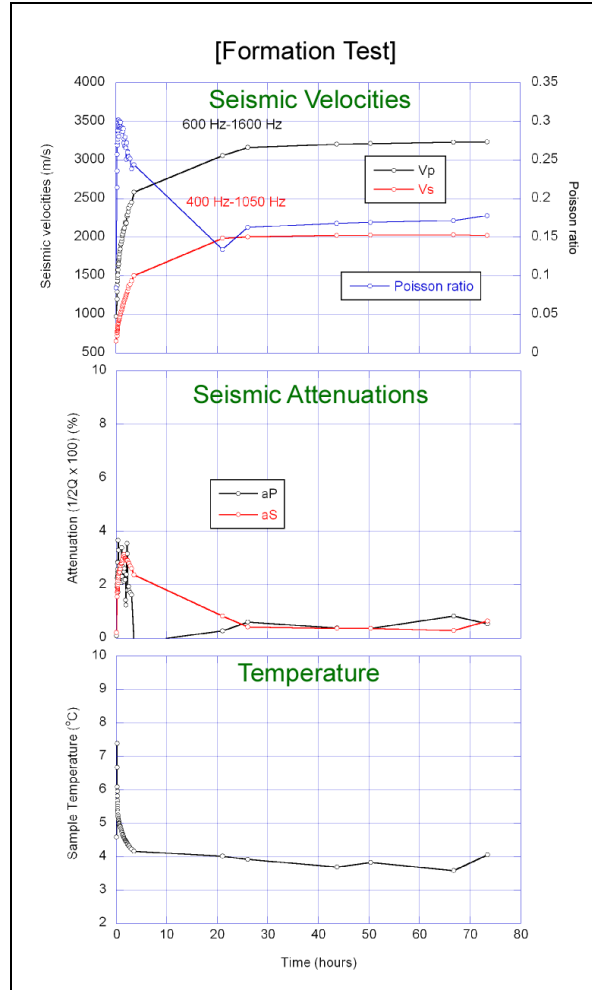


Figure 8. Seismic property changes over time during the CH₄ hydrate formation test

Gas Exchange

Pressure, Temperature, Differential Pressure

A mixture of 23% CO₂, 77% N₂ was flowed through the CH₄-hydrate-bearing sample at a flow rate of 0.5 mL/min (roughly 0.88 pore volumes per hour). This was accomplished using a high-pressure syringe pump running in the constant pressure mode upstream, and another high-pressure syringe pump downstream running in a constant flow withdrawal mode at 0.5 mL/min. The upstream pump continuously seeks the desired pressure (varying ~ 1 psi about 1400 psi), inducing some variability into the differential pressure data. For this reason, a 20 period (20 second period) moving average line (black line in Figure 9) is also displayed for the differential pressure data. The largest variations in the differential pressure data (yellow arrow in Figure 9) are artifacts of gas sampling when flow was momentarily stopped (~3 seconds). Like the other variations, these were short-lived. It is interesting to note that while the permeability at the beginning of the test was similar to the CH₄ hydrate permeability, as the test progressed, the permeability increased (decrease in differential pressure), however it decreased notably every time the sample was shut in to refill the pumps. The bath temperature (brown line in Figure 7)

was relatively constant, yet the sample temperature responded in a buffered fashion to the room temperature. There was no obvious temperature response to the change in influent gas chemistry. At one point (brown arrow in Figure 9), we lowered the bath temperature to check the hypothesis that these mild temperature variations were causing large variations in sample resonance (more below).

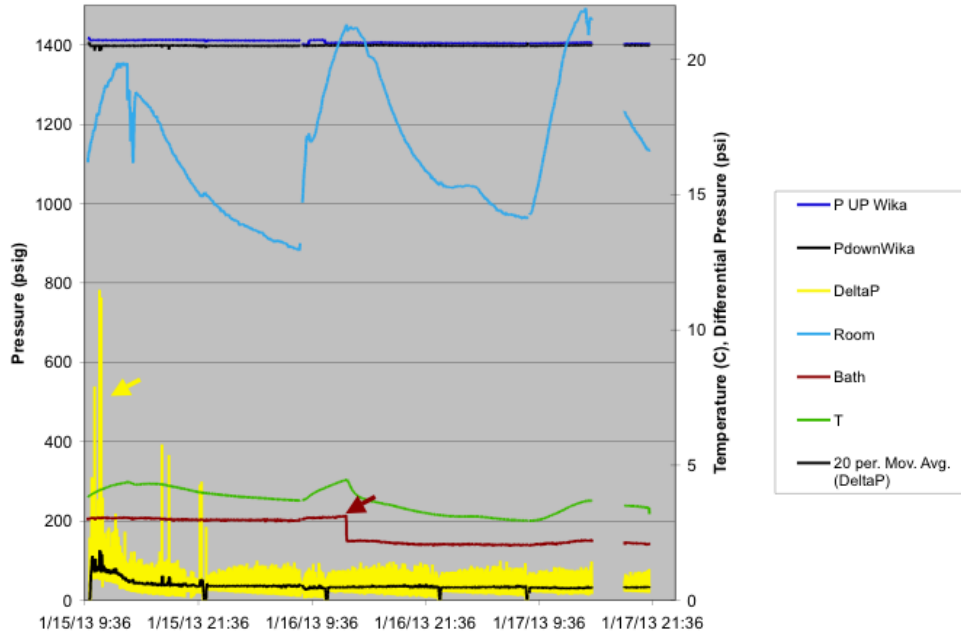


Figure 9. Physical conditions during gas exchange

Gas Composition

As expected and similar to the tests reported above, the effluent gas stream initially was composed purely of CH₄ as the CH₄ was flushed from the sample. Although simultaneous gas exchange with hydrate was occurring (see resonance section below) it could not be detected chemically until the gas reached the sample point. The N₂ and CO₂ concentrations increased over time with declining CH₄ concentration. After several pore volumes of the mixed gas were flowed, a spike in CH₄ concentration occurred (from 3.6% to 9.4% over 40 minutes). This was concurrent with a gradual temperature increase in the sample (3.6C to 4.3C over several hours). This temperature shift corresponds with room temperature changes, but further deconvolution of the data may show a gas-exchange related temperature change. Other temperature increases and decreases occurred as well without drastic gas composition changes. The next most significant temperature increase (3.8C to 4.2C on the following day) resulted in a CH₄ concentration increase from 0.2% to 0.4%.

The volumes of gas injected and recovered did not match each other (Figure 10, brown and blue lines). This could mean 1) the volume indicators are inaccurate, 2) a leak from the confining N₂ is present, and/or 3) a change in gas chemistry has occurred. The accuracy of the volume indicators is being verified. A leak from the confining N₂ would

have become evident during other parts of the test, as the sample was shut in many times and no obvious pressure increase was recorded. The molar densities of the gases at 18C are: CH₄ (1414 psia) 4.8 mol/L, N₂ (1414 psia*0.77 = 1089 psi) 3.12 mol/L, and CO₂ (1414 psia*0.23 = 322 psi) 1.07mol/L. The summed N₂ and CO₂ densities are 4.19 mol/L, which is significantly lower than the CH₄ density. (This assumes ideal gas properties, which induce an error into the calculations.) The collected gas would be richer in CH₄, thus lower volume. Further analysis is needed to verify these alternative explanations.

The rate of gas exchange once the initial CH₄ peak had passed through the system, declined with time as the CH₄ was exchanged out. The average rate following the yellow arrow in Figure 10 ranged from 3.5 to 0.8 x 10⁻⁷ moles CH₄/(mole water*s), and the average value was 2.7 x 10⁻⁷ moles CH₄/(mole water*s).

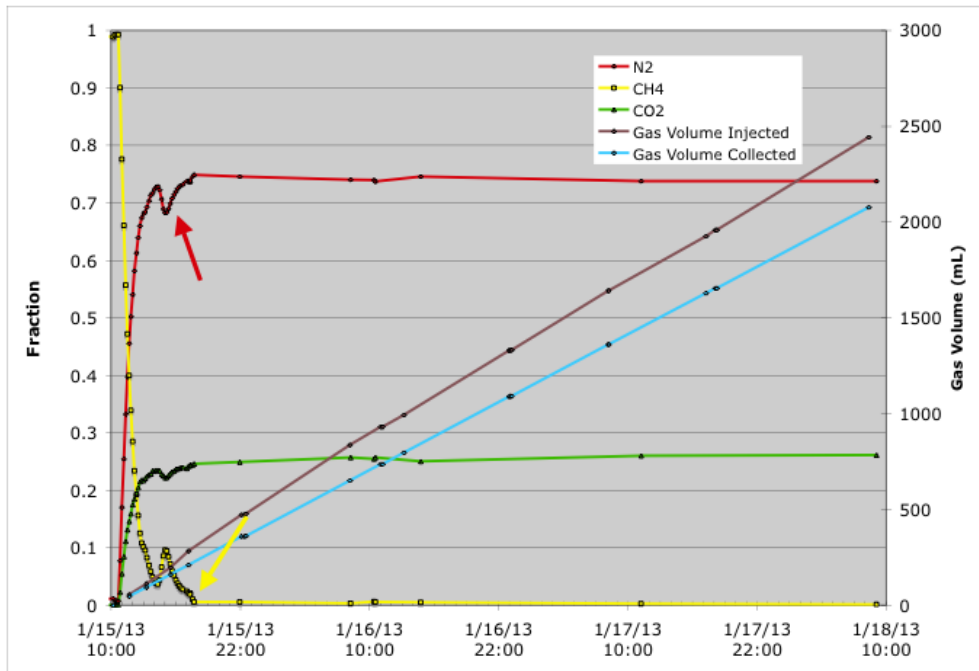


Figure 10. Effluent gas composition during gas exchange.

Seismic properties

Immediately after the CH₄ hydrate formation test, the CH₄-hydrate to CO₂-hydrate replacement test was conducted (Figure 11). Upon introducing the mixed N₂ (77%)-CO₂ (23%) gas was introduced in the sample, large decreases in seismic velocities and large increases in attenuations were observed. A slight increase in the Poisson ratio was also observed (from 0.18 to 0.2) but the change was very small. The decreases in velocities were up to ~330 m/s for the P wave and ~240 m/s for the S wave, about 10% of the original velocities. Attenuations increased up to the same level as during the CH₄-hydrate formation test.

Note that during this experiment as mentioned above, there were rather large sample temperature fluctuations, mostly due to large room temperature changes in the laboratory (see Figure 9). The behavior of the sample seemed to be related to the temperature variation. During a large temperature increase (as indicated in pink in the figure), the set temperature of the temperature control bath was decreased to counteract the effect. This resulted in some recoveries in the seismic velocities and decreases in attenuation.

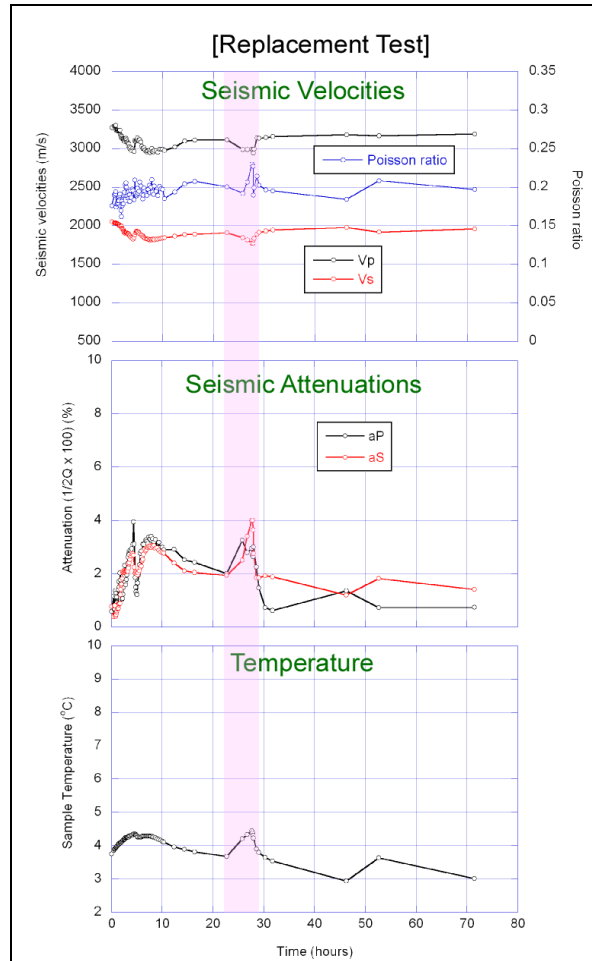


Figure 11. Seismic property changes during the CH₄-hydrate to CO₂-hydrate replacement test

Dissociation

Pressure, Temperature, Differential Pressure

Hydrate dissociation was accomplished by increasing the sample temperature by stepwise increasing the bath temperature (Figure 12). This resulted in a fairly constant rate of sample temperature increase. Differential pressure spikes shown in Figure 12 are the result of gas sampling. Elevated differential pressure resulting from rapid hydrate dissociation was not observed.

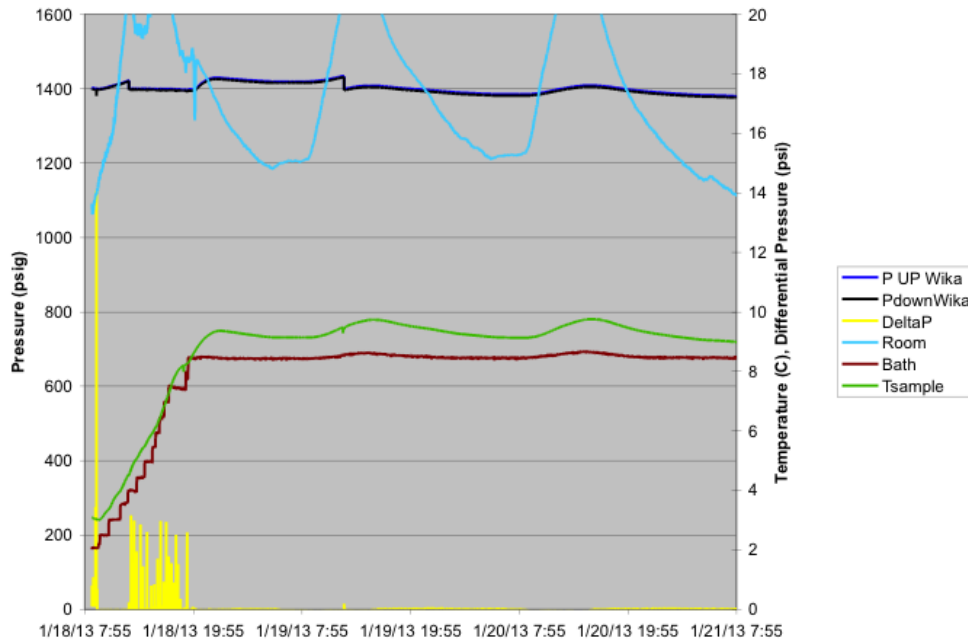


Figure 12. Temperature, pressure, and differential pressures during dissociation.

Gas Composition

The volume of gas produced and its composition are shown in Figure 13. Initially, the sample contained the mixed hydrate presumably in equilibrium with the inlet 23% CO₂ 77% N₂ gas. As dissociation occurred releasing CH₄ and CO₂, the N₂ concentration decreased. CO₂ was released preferentially to the CH₄ over the course of the dissociation. Whether that is the result of equilibrium processes for a uniform hydrate, or mass transfer limitations where a CO₂-rich hydrate layer overlies a CH₄-rich hydrate requires additional analysis. Ultimately, the produced gas fractions were 69% N₂, 24% CO₂, and 7% CH₄.

The dissociation was thermally induced, and the total pressure was held constant. Because N₂ is presumably not significantly held in the hydrate phase, dissociation of the hydrate - containing CH₄ and CO₂ - will dilute the N₂ and enrich the fraction (partial pressure) of the hydrate formers. If the hydrate were CO₂ hydrate in the CO₂/N₂ mixed gas, as the CO₂ becomes enriched (N₂ concentration becomes more dilute), the stability temperature increases (see Figure 14a). In our test, the N₂ was diluted by dissociation, thus the hydrate formers were enriched in the sample. This increased the hydrate stability temperature as the dissociation continued. This is compared to the N₂/CO₂ system in Figure 14b.

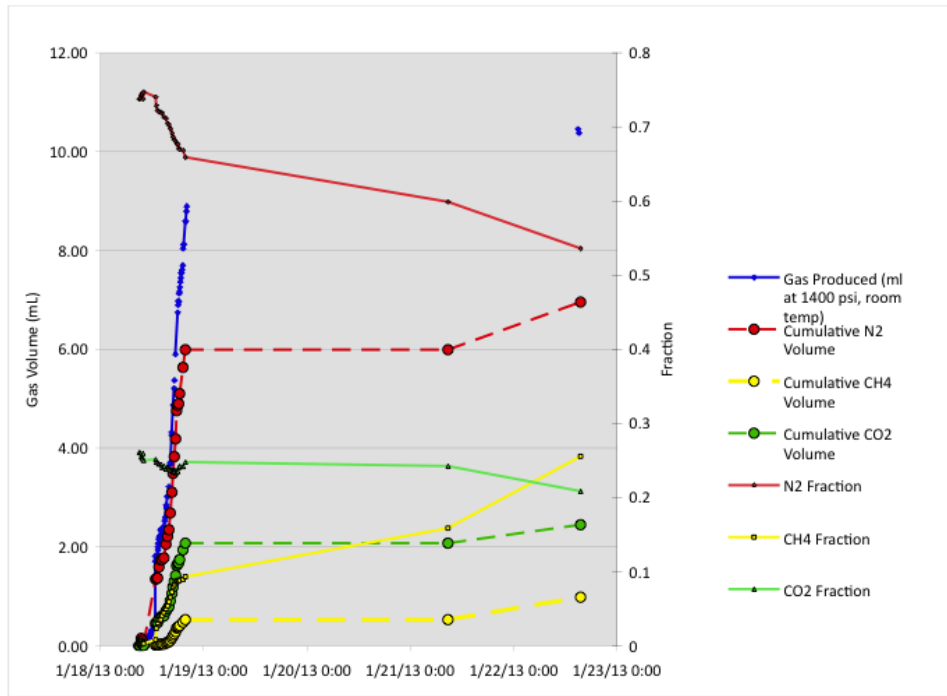
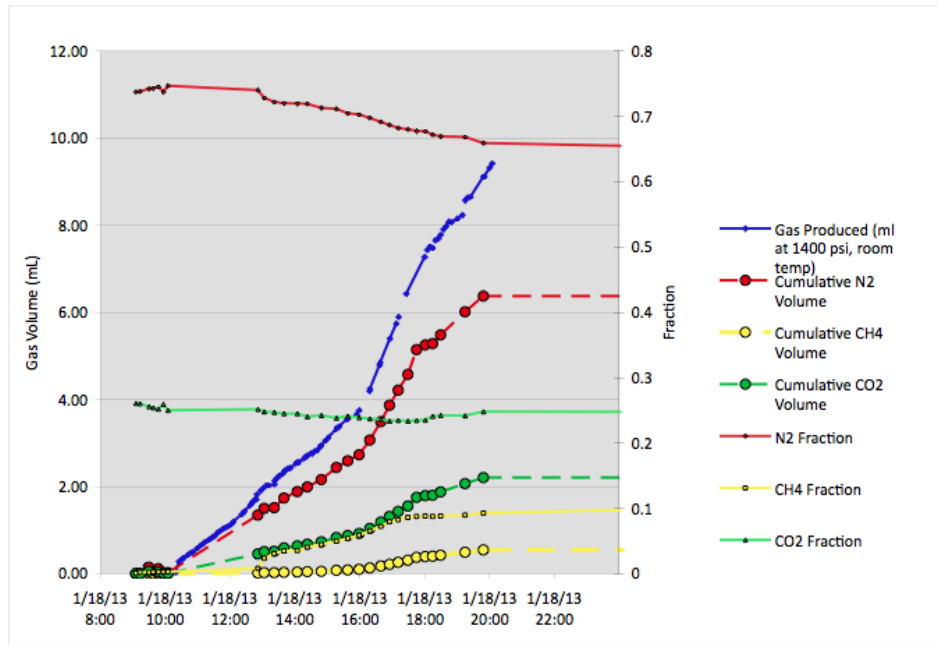
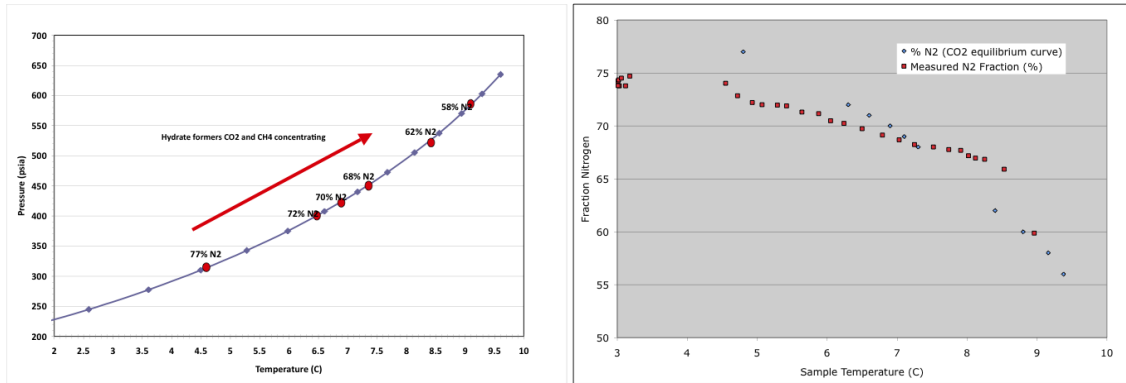


Figure 13. Volume of gas produced and gas composition. top: first 20 hours, bottom: whole test.



a. Figure 14. a. CO₂ stability curve showing N₂ composition for the 23% CO₂/77% N₂ mixture at 1400 psi. b. Comparison of extracted CO₂ hydrate equilibrium curve from a. to the observed temperature and gas chemistry.

Seismic properties

Dissociation of the mixed CH₄-CO₂ hydrate was conducted by increasing the sample temperature at a rate of approximately 0.5°C/hour (Figure 12). During the test, the seismic velocities decreased continuously until they reached the original velocities of the moist sand pack (Figure 15). In contrast, extremely large attenuations were observed, which peaked at 5–6 hours after the start of the test. The maximum attenuations were ~8–10% for the P wave and ~6.5% for the S wave. The Poisson ratio exhibited a small increase which peaked when the maximum attenuation occurred, and then decreased to the level for the original sand pack.

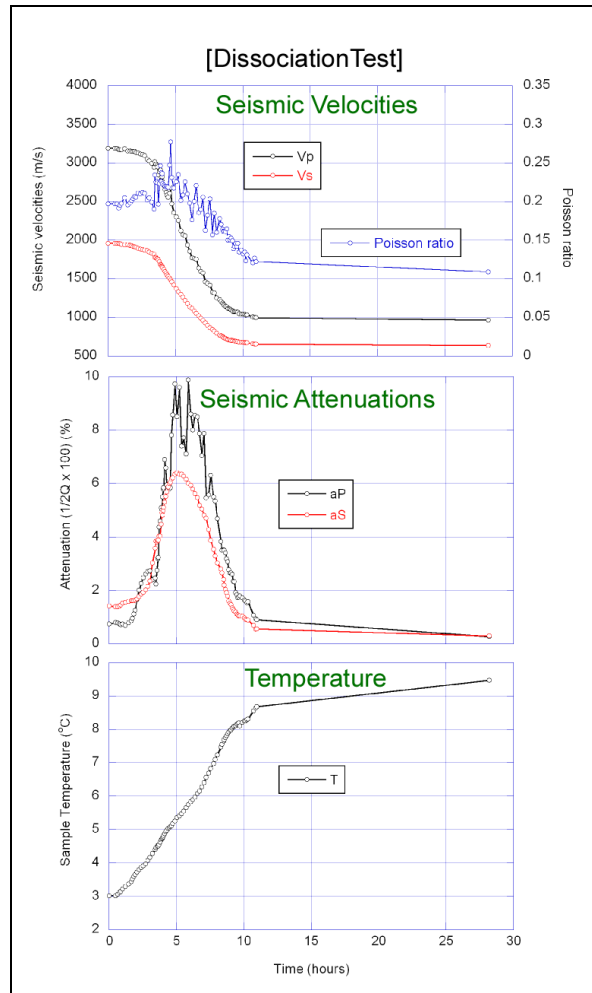


Figure 15. Seismic property changes over time during the mix-hydrate dissociation test

X-ray computed tomography

X-ray computed tomography was used to monitor the spatial density distribution over the range of experiments. Scanning was performed while the sample was moist sand, after CH₄ hydrate formed, after gas exchange, and at intervals during dissociation. An example is shown in Figure 16 showing the density distribution for the moist sand case. Changes during the different stages of the experiment were typically relatively small (Figure 17, in Hounsfield Units) but within the expected ranges of values.

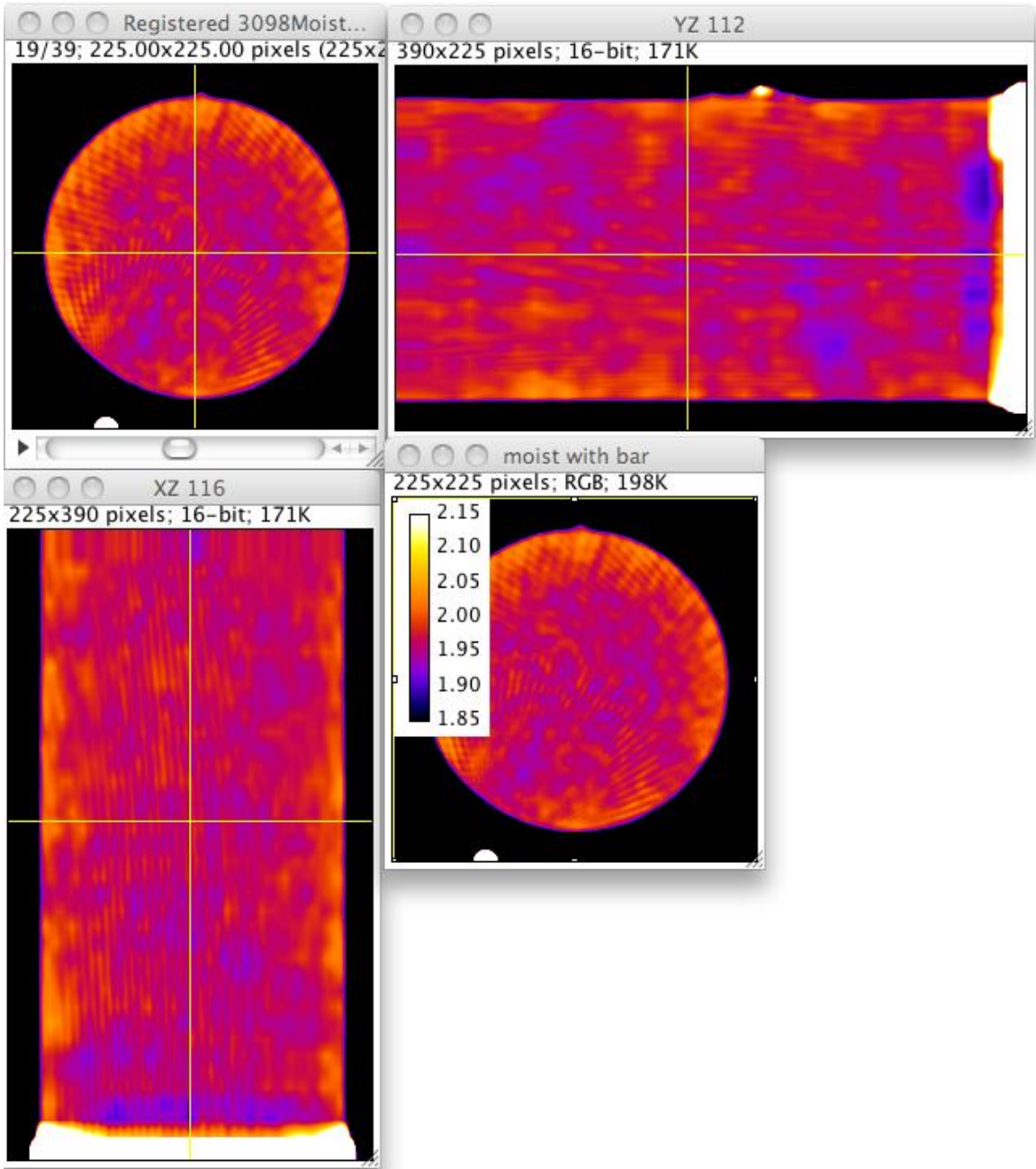


Figure 16. Density distribution for the moist sand sample. Upper left is a cross section in the center of the sample, upper right and lower left are perpendicular cross sections along the axis, and the lower right image shows the color bar.

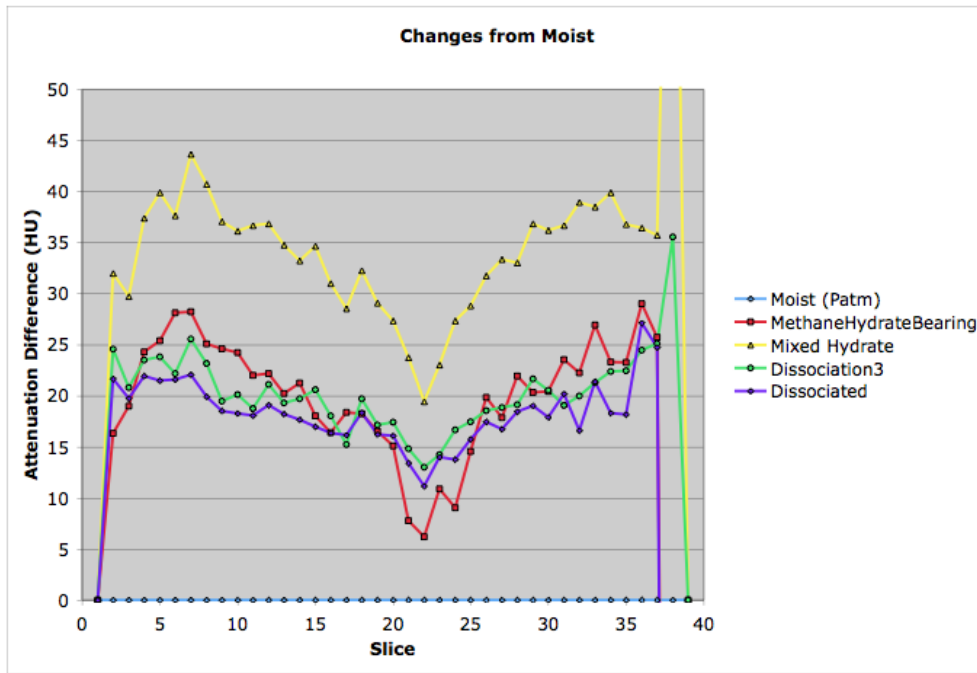


Figure 17. Density changes from the moist case. In a linear calibration, 1000 Hounsfield units is 1 g/cm³.

Discussion

Of the tests performed under this task, three are reported on here. Two of these tests were performed in long narrow columns (25:1 aspect ratio) and one in a short column (2:1 aspect ratio). Two tests were performed with an initial water saturation of 20%, and one with an initial water saturation of 40%. One test has a large suite of measurements made, while the others had a limited suite of measurements. The key observations from the tests were:

- 1) Permeability increased in some tests, and decreased in another. The permeability changed over the course of a set of measurements indicating physical changes in the porespace in the hydrate-bearing sands.
- 2) The gas exchange rates following the CH₄ peaks ranged from about 3.8×10^{-7} moles CH₄/(mole water*s) to 5×10^{-8} moles CH₄/(mole water*s), where the moles water refers to the water held in hydrate.
- 3) The CH₄ hydrate, when exposed to the 77% N₂ 23% CO₂ gas experienced dissociation and physical property changes.

In both of our tests not having the geophysical measurements, permeability decreased because of gas exchange. This was not the case for the test undergoing the suite of geophysical measurements which showed increasing permeability indications. In this test, several constrictions were present making true permeability measurements very difficult.

The permeability varied over the course of the test, with short shut-in times during which pumps were refilled causing permeability increases.

Gas exchange rates were computed for times following the CH₄ peak passing through the system. Additional information may be present in the breakthrough curves which may be brought forward during additional analysis. The rates were similar for all the tests, and declined over time. The rate reduction as time progressed would be expected as the amount of CH₄ in the sample would decrease over time. It should be pointed out that the rates presented here are subject to mass transfer limitations and flow preferential paths as would also be expected in a field test.

The sudden decreases in seismic velocities and particularly the increases in attenuations during the hydrate replacement test indicate that the CH₄-hydrate in the pore space was dissociating, and liquid water was being produced at the grain contacts. However, the small increases in the sample temperature, although it never exceeded the theoretical temperature for the stability of CO₂ hydrate, may have some impact on the dissociation.

To gain a better understanding of the process occurring within the sample, seismic velocities are plotted against the temperature (Figure 18). In this figure, velocities during the hydrate replacement test are shown as the path 1→2→3, and the dissociation test as 3→4→. Initially, the velocities decreased rapidly over a 0.5°C increase in the temperature of the sample (1→2). When the sample temperature was forced to decrease, some of the lost velocities were recovered (2→3). Interestingly, several small excursion loops due to fluctuating sample temperature and resulting changes in velocities all appear to collapse on single temperature-velocity curves. Further, for the early part of the dissociation test (3→4), the observed temperature-velocity behavior is in very good agreement with these curves. These results indicate that there is a phase boundary between the mixed hydrate and the mixed gas with the composition used in the experiment. Along this boundary, the effects of the mixed hydrate formation and dissociation seem to be reversible.

During hydrate dissociation, a range of stable states was encountered. As the temperature increased, the gas composition adjusted itself so that a new equilibrium state was obtained. This resulted in temperatures from over 4 to about 9 having some stable hydrate, and strongly buffered dissociation.

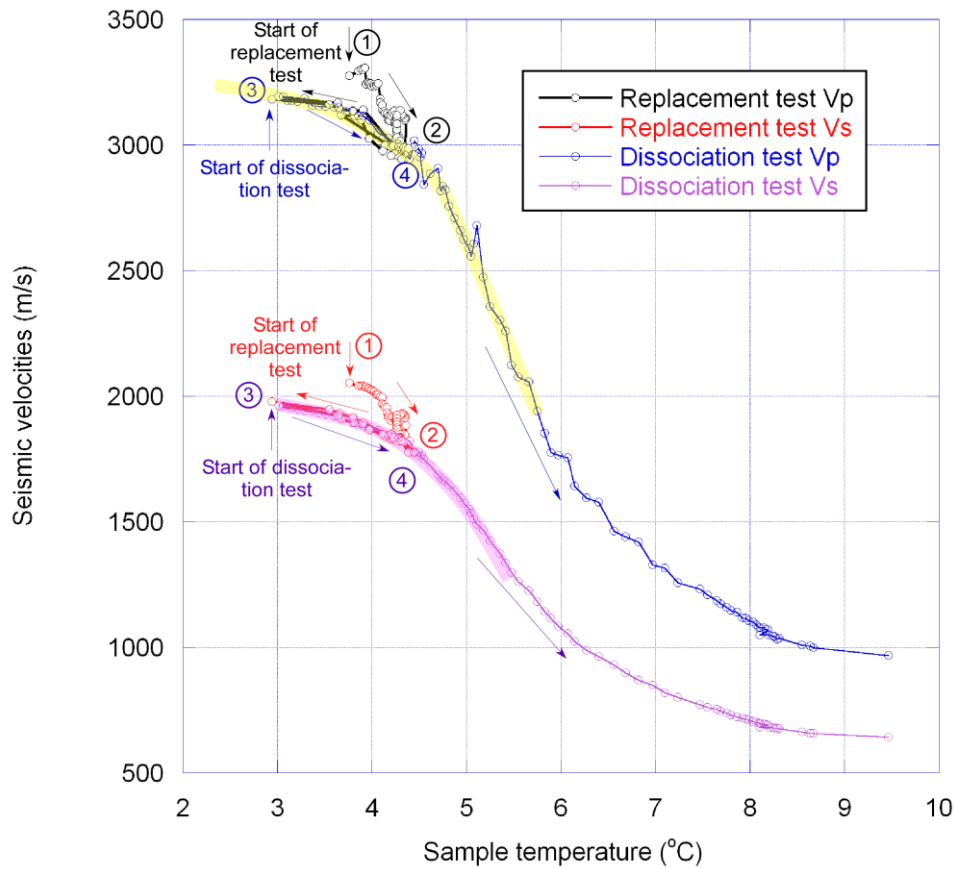


Figure 18. Seismic velocities during the gas exchange test plotted against sample temperature.

Risk Analysis

Risks associated with FWP task execution include safety risks, personnel availability risks, risks of equipment failure, facility risks, and technical uncertainties. Each will be addressed separately.

The proposed studies require the use of compressed gases and the use of flammable gases. LBNL has worked safely on similar projects in the past, and has a good track record for safety. Safety risks are minimized by using appropriately sized and rated pressure vessels and lines, small volumes when possible, carefully considered techniques, and appropriate safety oversight and monitoring. The consequences of the safety risks include personal injury, equipment damage, and schedule delays. To date, these risks have been managed well causing no injuries or delays.

Personnel who will be working on this project are committed to providing a best effort to perform project tasks and meet the project schedule. None of the personnel working on this project are solely funded by this project, however, and consequently are required to meet schedule and availability requirements of other projects that are not always known at project inception. Additionally, factors such as illness and jury duty can impact project

schedule. Planning and communication among project personnel is underway to minimize the impact of scheduling conflicts.

Some of the equipment used in this research is expensive, specialized, and/or one-of-a-kind. Although not anticipated, equipment can fail and repair/replacement can be expensive and time consuming. Currently, all needed equipment is functioning properly, and is scheduled to be available.

Facility risks include facilities not being available to allow performance of the work. During the performance period of this FWP, the laboratories and offices of project participants will move to a newly remodeled building. This entails shutting down and dismantling systems, moving, reassembling systems in the new laboratory, and testing, restarting and recalibrating the equipment. Additionally, since most safety documentation at LBNL is location dependent, modification and approval of the new documentation will be required. Planning is underway to minimize the facility risks. Significant delays occurred due to a changing laboratory move schedule. These occurred because move preparations occurred, resulting in idling equipment, reestablishing function and permits, and restarting test sequences over a range of projects.

Technical uncertainties result from research tasks because often the results of a research step are unexpected requiring changes in subsequent research steps. Although these unexpected results often result in changes in the schedule and budget, the lessons learned from the results are often valuable. Several of these occurred during preliminary tests resulting in improved techniques.

Milestone Status

This report is the second of two milestone reports. The first milestone report was planned to be submitted on July 31, 2012 and was submitted on August 7, 2012. The original planned submission date for this report date was October 31, 2012, however this date was later modified to be January 31, 2013. This date slipped due to laboratory move related issues including deactivation and reactivation and repermitting of the X-ray CT scanner.

Schedule Status

As reported above, this milestone report was submitted after the planned submission date. The final results of this project will be presented in March 2013 at a meeting in Houston TX. Further data analysis is required to prepare the work for presentation and publication, and budget is available for this work.

Cost Status

Through December 31, 2013, \$45K of the funding awarded for this work has been spent. This was augmented at the beginning of the project with \$8K carryover funding from previous DOE/NETL gas hydrate work, therefore total expenses on this project have been \$53K. This is less than the \$99K spending anticipated to occur prior to December 31,

2012, but anticipated because of schedule delays. Expenditures in the current quarter to date are \$27K, resulting in \$80K spent on the project to date. The remaining funds will be used to to attend the meeting in Houston to discuss the ConocoPhillips project which this supplies data for, further data analysis, and for publication.

Cost Plan/Status

Baseline Reporting Quarter		Year 1 Start: End:				Year 2 Start: End:			
		Q1	Q2	Q3	Q4	Q1	Q2*	Q3	Q4
Baseline Cost Plan									
Federal Share	Task1			3	3	3	1		
	Task2			14	14	14			
	Task3			12	20	16			
Non-FederalShare				0	0	0	0		
Total Planned Cost				29	37	33	1		
Federal and Non-Federal				29	37	33	1		
Cumulative Baseline Cost				29	66	99	100		
Actual Incurred Costs									
Federal Share	Task1			1	3	3	3		
	Task2			0	34	10	7		
	Task3			0	2	1	36		
Non-FederalShare									
Total Planned Cost				29	37	33	1		
Federal and Non-Federal									
Cumulative Incurred Cost				1	40	54	100		
Variance									
Federal Share	Task1			-2	0	0	2		
	Task2			-14	20	-4	7		
	Task3			-12	-18	-15	36		
Non-FederalShare									
Total Planned Cost									
Federal and Non-Federal									
Cumulative Variance				-28	-26	-45	0		

Table 1. Cost plan and status. * indicates current quarter estimated expenses.

Conclusions

- The introduction of a 77%N₂/23%CO₂ gas into methane hydrate at 4C and 1400 psig results in hydrate dissociation and water formation. This was indicated by geophysical monitoring of our sample, and both V_p and V_s decreased and attenuation increased dramatically. The full impacts of this sample softening are unclear because the wave speeds did not decrease to the initial moist sand condition.

- The rate of gas exchange decreases over time as methane is exchanged out of the hydrate, and/or becomes occluded from the gas flow by converted hydrate. Rates of gas exchange were on the order of 10^{-7} moles CH₄/(mole water*s).
- Slow hydrate dissociation occurred over a wide range of stability conditions resulting from the concentration of the hydrate forming gases.

References

- Adisasmito, S., Frank, R.J. and Sloan, E.D., 1991. Hydrates of carbon dioxide and methane mixtures. *Journal of Chemical & Engineering Data*, 36(1): 68-71.
- Anderson, R., Llamedo, M., Tohidi, B. and Burgass, R.W., 2003. Experimental Measurement of Methane and Carbon Dioxide Clathrate Hydrate Equilibria in Mesoporous Silica. *The Journal of Physical Chemistry B*, 107(15): 3507-3514.
- Goel, N., 2006. In situ methane hydrate dissociation with carbon dioxide sequestration: Current knowledge and issues. *Journal of Petroleum Science and Engineering*, 51(3,Äi4): 169-184.
- Lee, H., Seo, Y., Seo, Y.-T., Moudrakovski, I.L. and Ripmeester, J.A., 2003. Recovering Methane from Solid Methane Hydrate with Carbon Dioxide. *Angewandte Chemie International Edition*, 42(41): 5048-5051.
- Lee, M.W. and Collett, T.S., 2005. Controls on the physical properties of gas hydrate-bearing sediments because of the interaction between gas hydrate and porous media, Fifth International Conference on Gas Hydrates, Trondheim, Norway, pp. 2014.
- Linga, P., Kumar, R. and Englezos, P., 2007. Gas hydrate formation from hydrogen/carbon dioxide and nitrogen/carbon dioxide gas mixtures. *Chemical Engineering Science*, 62(16): 4268-4276.
- Lu, H., Tsuji, Y. and Ripmeester, J.A., 2007. Stabilization of methane hydrate by pressurization with He or N₂ gas. *Journal of Physical Chemistry B*, 111: 14163-14168.
- Nago, A. and Nieto, A., 2011. Natural Gas Production from Methane Hydrate Deposits Using CO₂ Clathrate Sequestration: State-of-the-Art Review and New Technical Approaches. *Journal of Geological Research*, 2011.
- Nakagawa, S., 2011. Split Hopkinson resonant bar test for sonic-frequency acoustic velocity and attenuation measurements of small, isotropic geological samples. *Review of Scientific Instruments*, 82(4): 044901-13.
- Ota, M., Abe, Y., Watanabe, M., Smith Jr, R.L. and Inomata, H., 2005a. Methane recovery from methane hydrate using pressurized CO₂. *Fluid Phase Equilibria*, 228,Äi229(0): 553-559.
- Ota, M. et al., 2005b. Replacement of CH₄ in the hydrate by use of liquid CO₂. *Energy Conversion and Management*, 46(11,Äi12): 1680-1691.
- Ota, M. et al., 2007. Macro and microscopic CH₄-CO₂ replacement in CH₄ hydrate under pressurized CO₂. *AIChE Journal*, 53(10): 2715-2721.

- Park, Y. et al., 2006. Sequestering carbon dioxide into complex structures of naturally occurring gas hydrates. PNAS, 103(34): 12690–12694.
- Seo, Y.-T., Lee, H. and Yoon, J.-H., 2001. Hydrate Phase Equilibria of the Carbon Dioxide, Methane, and Water System. Journal of Chemical & Engineering Data, 46(2): 381-384.
- Stevens, J.C. et al., 2008. Experimental hydrate formation and gas production scenarios based on CO₂ sequestration, 6th International Conference on Gas Hydrates (ICGH 2008), Vancouver, British Columbia, CANADA.
- Zhao, J. et al., 2012. A Review on Research on Replacement of CH₄ in Natural Gas Hydrates by Use of CO₂. Energies, 5(2): 399-419.

National Energy Technology Laboratory

626 Cochrans Mill Road
P.O. Box 10940
Pittsburgh, PA 15236-0940

3610 Collins Ferry Road
P.O. Box 880
Morgantown, WV 26507-0880

13131 Dairy Ashford Road, Suite 225
Sugar Land, TX 77478

1450 Queen Avenue SW
Albany, OR 97321-2198

Arctic Energy Office
420 L Street, Suite 305
Anchorage, AK 99501

Visit the NETL website at:
www.netl.doe.gov

Customer Service Line:
1-800-553-7681

